Volume 16
Number 9
September 2023
Pages 3625–4106

Energy & Environmental Science

rsc.li/ees

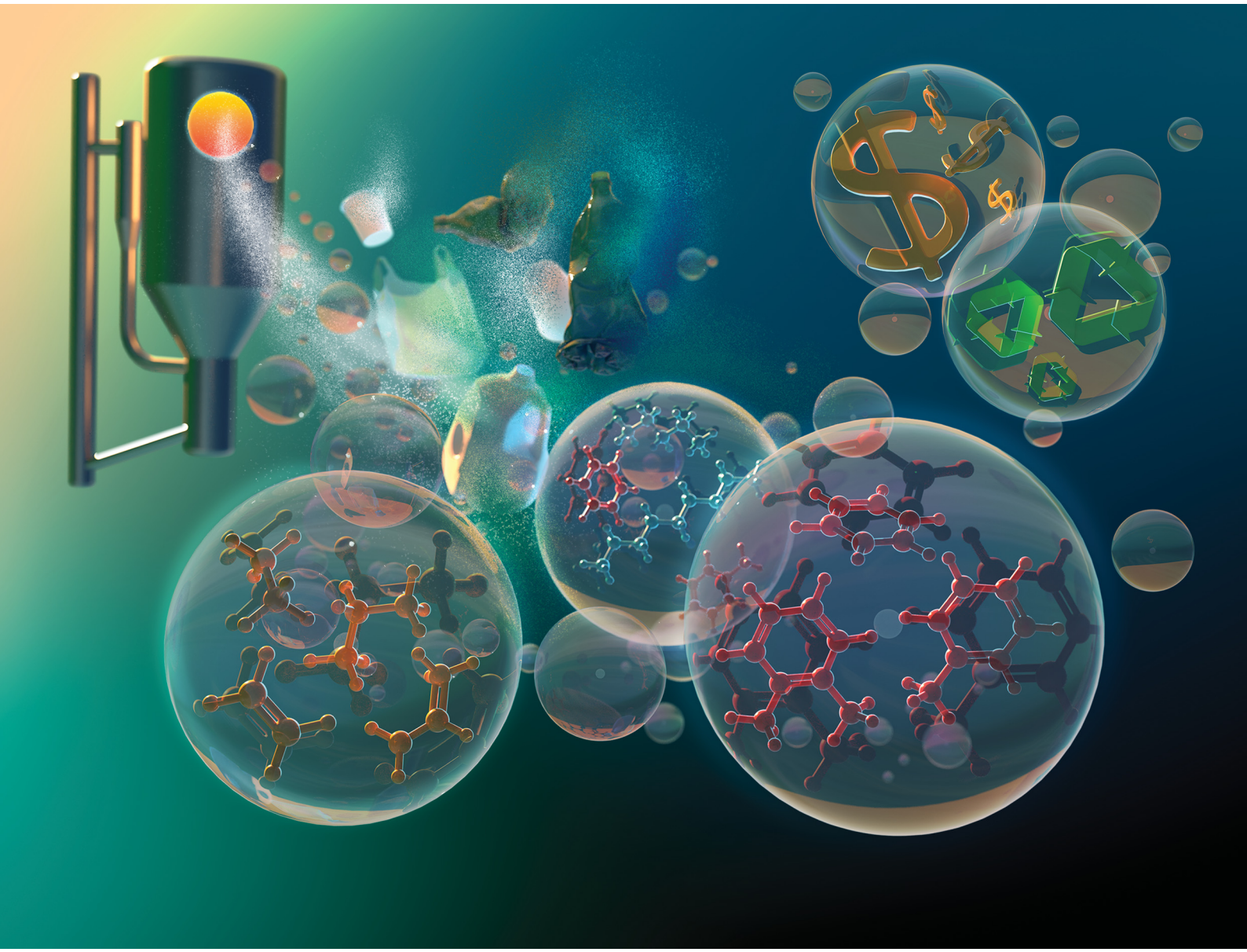

ISSN 1754-5706

ROYAL SOCIETY OF CHEMISTRY

ANALYSIS
Gregg T. Beckham *et al.*
Techno-economic analysis and life cycle assessment for catalytic fast pyrolysis of mixed plastic waste

Energy & Environmental Science

ROYAL SOCIETY OF CHEMISTRY

ANALYSIS

View Article Online
View Journal | View Issue

Cite this: *Energy Environ. Sci.*, 2023, **16**, 3638

Techno-economic analysis and life cycle assessment for catalytic fast pyrolysis of mixed plastic waste†

Geetanjali Yadav, [ab] Avantika Singh,*[ab] Abhijit Dutta, [a] Taylor Uekert, [bc] Jason S. DesVeaux, [ab] Scott R. Nicholson, [bc] Eric C.D. Tan, [a] Calvin Mukarakate, [a] Joshua A. Schaidle, [a] Cody J. Wrasman, [a] Alberta C. Carpenter, [bc] Robert M. Baldwin, [bd] Yuriy Román-Leshkov [be] and Gregg T. Beckham *[bd]

Pyrolysis of waste plastics has gained interest as a candidate chemical recycling technology. To examine the potential of this approach, we conducted a techno-economic analysis (TEA) and life cycle assessment (LCA) of a conceptual catalytic fast pyrolysis (CFP) facility that converts 240 metric tons/day of mixed plastic waste. The modeled base case predicts the minimum selling price (MSP) of a benzene, toluene, and xylenes (BTX) mixture at $1.07 per kg when co-products are sold at their average market prices. We predict that the aromatic product stream can be cost-competitive with virgin BTX mixtures ($0.68/kg) if the mixed waste plastics are available for less than $0.10/kg or if crude oil prices exceed $60/barrel. Moreover, we estimate that CFP-based conversion of waste plastics can reduce the total supply chain energy use by 24% but with a 2.4-fold increase in greenhouse gas (GHG) emissions per kilogram of BTX, relative to incumbent manufacturing process. Sensitivity analysis highlights that feedstock cost, co-product selling prices, capital cost for product separations, and operating costs are key cost drivers. Further, we examine three additional CFP processes that differ in product composition, namely naphtha, and a case where the products are rich in either C_2–C_4 olefins or BTX aromatic hydrocarbons. Whereas the MSP of naphtha ($2.18/kg) is ~4-fold higher than virgin naphtha, both the olefin-rich and aromatics-rich product cases exhibit a potential reduction in MSP up to 40%, with a 21%–45% reduction in total supply chain energy and 2.2–3.8-fold increase in GHG emissions relative to incumbent manufacturing processes. LCA predicts that the CFP process exhibits lower fossil fuel depletion than virgin manufacturing across all cases as well as lower acidification, ozone depletion, and smog formation for select cases, but high utility and feedstock preparation requirements result in poorer performance across other metrics. Overall, this study highlights important process parameters for improving CFP of mixed waste plastics from economic and environmental perspectives.

Received 8th March 2023,
Accepted 2nd June 2023

DOI: 10.1039/d3ee00749a

rsc.li/ees

Broader context

Waste plastics represent a ubiquitous pollution problem. To enable waste plastics to become a useful feedstock, technological innovation will be required, especially for plastics for which no recycling infrastructure exists. Technologies to this end must be considered rigorously in comparison to one another with transparent process analyses. This study presents a detailed process analysis of a mixed plastic waste refinery employing catalytic fast pyrolysis as a conversion technology. The analyses determine key economic and environmental drivers and highlight potential solutions to improve the viability of plastics pyrolysis processes.

[a] *Catalytic Carbon Transformation and Scale-Up Center, National Renewable Energy Laboratory, Golden, CO, 80401, USA. E-mail: avantika.nrel@outlook.com*
[b] *BOTTLE Consortium, Golden, CO, USA. E-mail: gregg.beckham@nrel.gov*
[c] *Strategic Energy Analysis Center, National Renewable Energy Laboratory, Golden, CO, 80401, USA*
[d] *Renewable Resources and Enabling Sciences Center, National Renewable Energy Laboratory, Golden, CO, 80401, USA*
[e] *Department of Chemical Engineering, Massachusetts Institute of Technology, Cambridge, MA, 02142, USA*

† Electronic supplementary information (ESI) available. See DOI: https://doi.org/10.1039/d3ee00749a

Introduction

Waste plastics are rapidly accumulating in both landfills and the natural environment.[1,2] Mechanical recycling is currently the most prevalent recycling technology, but it is mostly limited to polyethylene terephthalate (PET) bottles and some forms of high-density polyethylene (HDPE).[3,4] This limitation has prompted the development of new recycling methods ranging from improved mechanical recycling to chemical recycling.[5–12]

Among chemical recycling technologies, pyrolysis is one of the few methods that can deconstruct mixed plastics across a broader slate of polymers than those currently eligible for mechanical recycling.[13–18] Pyrolysis of mixed plastic waste occurs at temperatures from 300 °C–700 °C in the absence of oxygen, and the process typically produces a hydrocarbon-based liquid, solid char, and light gases.[18,19] The hydrocarbon products may be used to create monomers for new plastics or other chemicals, refined to fuels, or some combination of these options.[20] Mixed waste plastics, especially those rich in polyolefins, are a potentially suitable feedstock for pyrolysis because they are inherently difficult to separate, and produce olefinic and aromatic hydrocarbons *via* pyrolysis due to their high carbon content and relatively low oxygen content.[21] Given that fast pyrolysis of plastics produces a mixture of olefinic and paraffinic hydrocarbons with a broad range of carbon numbers C_1–C_{60}^+, catalysts are often used to narrow the product distribution and increase yields of target products.

Catalytic fast pyrolysis (CFP) has been studied for plastics as a function of catalyst type and loading, temperature,[22,23] residence time,[24] heating rate,[25] reactor configuration,[26] and other variables.[4,22,23,27–29] CFP of plastics generates a suite of products with yields that depend on the process configuration and catalyst, including aromatics (10–70 wt%),[30,31] olefins (20–80 wt%),[4,29,32,33,34] and naphtha (15–90 wt%).[35–38] The mixture of products from these processes requires separations to be fungible with fuels, or these mixtures can be integrated into the existing petrochemical complex.[39–43]

There is growing interest in assessing the economic and environmental implications of pyrolysis of waste plastics. While several analyses have examined plastic pyrolysis refineries, highlighting the impact of plant size, feedstock type and quantity, operating conditions, and products,[44–50] there is a need for a comprehensive, transparent techno-economic analysis (TEA) and life cycle assessment (LCA) of mixed plastic waste pyrolysis to produce fuels and chemicals.[20] To that end, here we develop a process model for a mixed plastics waste refinery that employs feedstock pre-processing, CFP, and product separation to naphtha, C_2–C_4 olefins, and BTX aromatic hydrocarbons. Because of the vast experimental literature on plastics pyrolysis, we were able to model a conceptually feasible plant design. Sensitivity analysis evaluating process modifications was used to identify key drivers of cost, energy, and greenhouse gas (GHG) emissions. The material flows through industry (MFI) tool was used to compare the energy and GHG emissions impacts of CFP-derived products with those of virgin manufacturing processes.[51] SimaPro was used to quantify the environmental impacts of different products derived from the pyrolysis of mixed plastic wastes through LCA, and the results were compared to incumbent processes.[20]

Results

Process description and model assumptions

A process model for the conversion of mixed plastic waste to petrochemicals was developed in Aspen Plus V10 and used as the basis for TEA and LCA. Details of the design assumptions, process configurations, and operating conditions are described in the ESI.†

Four scenarios were modeled, for which the stream mass flows are shown in Fig. 1. The "Case A – naphtha product"

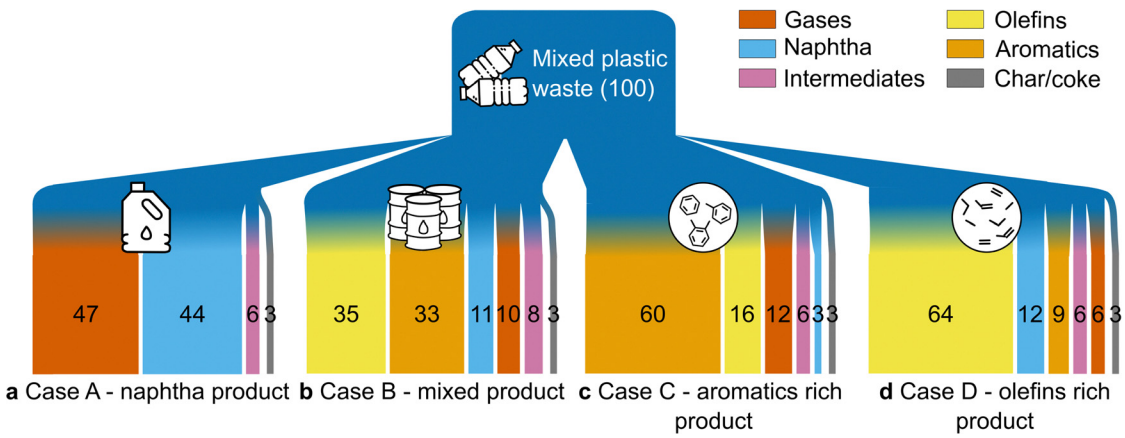

Fig. 1 Overview of product mass distributions across the four scenarios considered in this study. (a) Case A – naphtha product. Here, the hot effluent vapor stream from the pyrolysis section is quenched to yield a naphtha-rich liquid stream comprising gasoline-range, diesel-range, and high-boiling-point hydrocarbons (>370 °C). (b) Case B – mixed product. The vapor stream is quenched to separate an olefins-rich gaseous stream (total olefins yield = 35 wt%) and an aromatics-rich liquid stream (total aromatics yield = 33 wt%). (c) Case C – aromatics-rich product. The process design highlights the maximum production of aromatic chemicals of up to 60 wt% (trade-offs with olefins yield) using a catalyst-to-feed (C/F) ratio of 4. (d) Case D – olefins-rich product. The process diagram highlights the greater yield of olefins. The process intermediates including char and heavies are utilized to generate heat for the pyrolysis reactor operation in all the cases.

includes CFP of mixed plastics to a liquid naphtha-like stream (Fig. 1a).[52,53] The "Case B – mixed product" examines mixed plastics CFP with downstream product separation to produce naphtha, BTX aromatic compounds, and olefins (Fig. 1b). Two additional cases highlight the effect of catalyst selectivity to produce primarily BTX aromatic chemicals (Case C – aromatics-rich product, Fig. 1c) or C_2–C_4 olefins (Case D – olefins-rich product, Fig. 1d). Cases B, C, and D produce co-products, and credits are considered. The names of the respective cases are derived from the principal product for which the minimum selling price (MSP) is estimated. Key operating assumptions and yields for these cases are presented in Table 1, with additional details in the ESI.† The plant is modeled based on mature (*n*th) plant assumptions and product transportation costs are not included.

The process was modeled with a feedstock composition (Table S1, ESI†) of 39% low density polyethylene (LDPE), 24% polypropylene (PP), 19% HDPE, 11% polystyrene, 4% polyvinyl chloride (PVC), and 3% PET. This composition represents the average mixed stream at a materials recovery facility

Table 1 Operating assumptions for four CFP refinery designs. All four process designs employed processing of 240 TPD of mixed plastic feedstock into a bed of spent fluid catalytic cracking (FCC) catalyst and/or a zeolite catalyst in an *in situ* pyrolysis reactor coupled with a char combustor/catalyst regenerator[54–57]

Process area	Parameters	Case A – naphtha product	Case B – mixed product	Case C – aromatics-rich product	Case D – olefins-rich product
Operating conditions	CFP reactor temperature (°C)	550	670	670	670
	CFP reactor gauge pressure (bar)	3	3	3	3
	CFP reactor residence time (s)	<2	<2	2–4	1–2
Catalyst	Catalyst-to-feedstock (C/F) ratio (w/w)	6	6	4	28
	Catalyst	62.5 wt% spent FCC + 37.5 wt% ZSM-5 zeolite[54]	62.5 wt% spent FCC + 37.5 wt% ZSM-5 zeolite[54]	70 wt% spent FCC + 30 wt% ZSM-5 zeolite[55]	100 wt% spent FCC with ~1% rare earth oxide content[55]
In situ reactor	Feedstock conversion (wt%)	100	100	100	100
	Ratio of bed solids to dry plastic feed (w/w)	6	6	4	28
	Fluidizing gases to dry feed (w/w)	0.8	0.76	0.76	0.76
Combustor/ regenerator	Temperature (°C)	550	670	670	670
	Pressure (bar)	1	3	3	3
	Excess air (%)	10	15	15	15
	Solids temperature before transfer to CFP reactor (°C)	550	670	670	670
Primary product yield	Yield (kg kg^{-1} feedstock)	0.43	0.2	0.3	0.12
	Yield (million kg per year)	34	15.5	24	9.7
Mass percent of liquid products	Total yield (wt%)	50	50	69	31
	Gasoline (C_5–C_{12} hydrocarbon) (wt%)	44	44	63	20
	C_6–C_8 aromatics (% gasoline)	51	51	93	8
	C_9–C_{12} aromatics (% gasoline)	25	25	2.5	3
	Diesel (C_{12}–C_{15} hydrocarbon) (wt%)	5.1	5.1	5	10
	Heavies (C_{24}+ hydrocarbon) (wt%)	0.9	0.9	1	1
Mass percent of gaseous products	Total yield (wt%)	47	47	29	70
	Olefins (C_2–C_4 hydrocarbon) (wt%)	n.d.[c]	35	16	64
	Ethylene (%)	n.d.	7	3	16
	Propylene (%)	n.d.	16	7	35
	Butene(s)[a] (%)	n.d.	12	6	13
	Other gases (wt%)[b]	n.a.	12	13	6
Solid products	Coke/char (wt%)	3	3	2.5	3.2

[a] Consists of a mixture of *trans*-2-butene (2.9 wt%), 1-butene (2.08 wt%), *i*-butylene (4.9 wt%), *cis*-2-butene (2.2 wt%), and 1,3-butadiene (0.14 wt%). [b] Consists of a mixture of H_2, methane, CO, CO_2, and NGLs. [c] n.d. is not detected since these olefin rich gases are not separated in Case A – naphtha product.

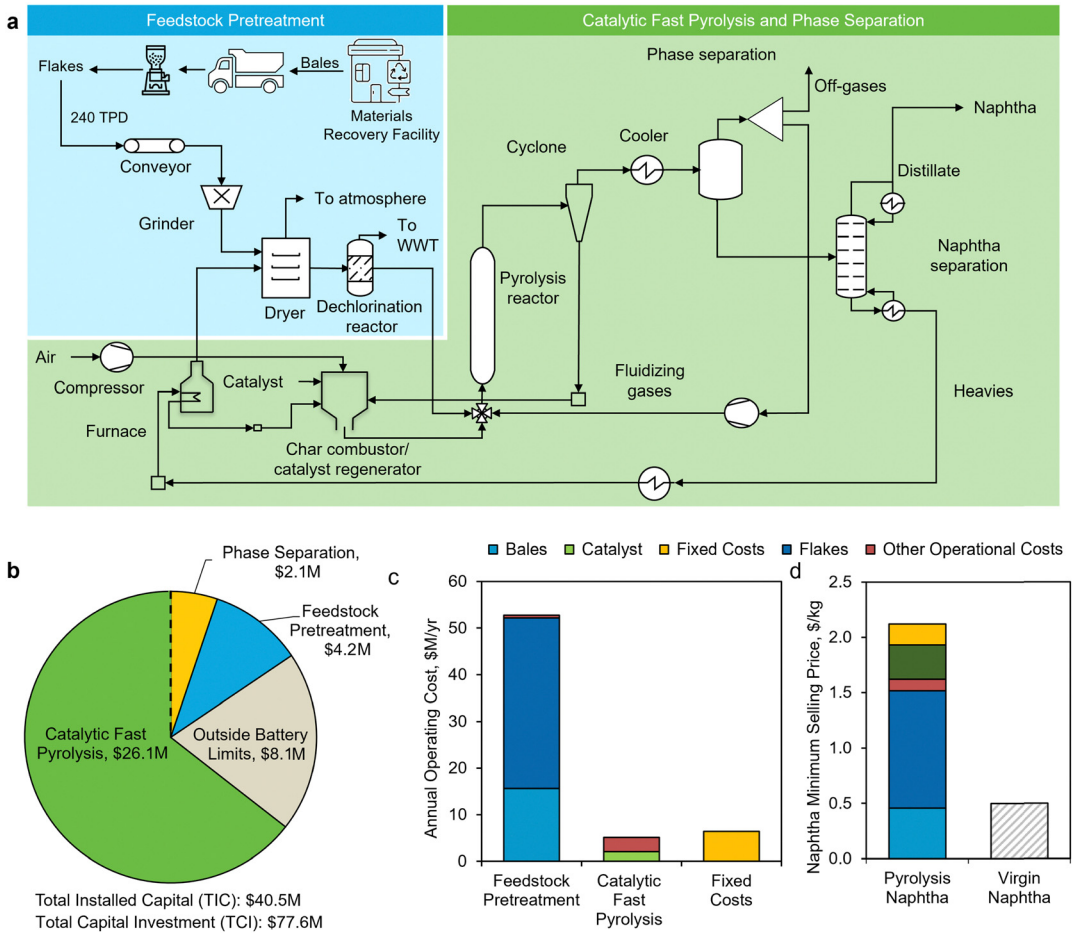

Fig. 2 TEA Results for Case A – naphtha product. (a) Process flow diagram of Case A. The pre-processed feedstock is catalytically pyrolyzed in an *in situ* fast pyrolysis reactor to produce a 50 wt% liquid naphtha stream that primarily contains gasoline (44 wt%) and diesel fractions. The aromatic content of the gasoline fraction is 76 wt%. (b) Capital cost breakdown by area for each process section, with a total installed capital (TIC) of $40.5 million and total capital investment (TCI) of $77.6 million. This includes $8.1M contribution assumed from the outside battery limits (OSBL) investment (OSBL is 25% of inside battery limits, ISBL), which consists of additional capital expenditure including piping and instrumentation required to integrate the over-the-fence utilities into the plant. (c) Annual operating expense by process section. Fixed costs include fixed variable expenses toward labor, maintenance, and property and insurance taxes. Other operational costs include utilities like process steam, cooling water, and natural gas for the operation of the facility. (d) MSP breakdown of the naphtha case. The MSP of naphtha from pyrolysis of mixed plastic waste is $2.18/kg, which is approximately 4-fold higher than that of fossil-derived naphtha ($0.50/kg).

(MRF)[47,48,58–60] in both the United States (U.S.) and European Union.[47,48,58,60] A baseline feedstock cost of $0.60/kg was used.[61] We modeled a 240-metric-ton-per-day (TPD) waste plastic processing capacity, consistent with a ~300-TPD facility currently under construction.[57,62] This is also approximately the average size of MRF in the U.S.[5,63] Overall, the annual processing capacity of a pyrolysis facility of this size represents 0.21% of total plastic waste generated in 2019 in the U.S.[60]

The mixed plastic feedstock bales are modeled to be procured from a MRF, where it will have undergone washing and removal of metal, wood, steel, glass, and paper. The mixed plastic bales are then transported to the waste plastic processing facility by truck (Fig. 2a).[64] Conveyor belts move the plastic feedstock to different pre-processing operations at the waste processing facility. The large bales of mixed plastic feedstock are converted to flakes (~25 mm). Next, two hammer mills connected in series further reduce the feedstock particle size to up to 2–3 mm diameter. Before the dechlorination step, any residual moisture in the feedstock is evaporated (<1% wet basis) by a dryer that utilizes hot flue gas from the plant. PVC is assumed to be the only polymer contaminant and is dechlorinated by thermal degradation (extrusion) at 300 °C prior to being fed to the pyrolysis reactor.[65,66]

Subsequently, the feedstock is converted to a hydrocarbon vapor using an *in situ*, dual-stage, circulating fluidized-bed reactor where catalyst particles function as the bed material for fluidization and as a heat transfer agent to deconstruct the waste plastics. Similar to an FCC unit in the refineries, the catalyst is regenerated in a separate combustion reactor, where coke is burned off at a higher temperature than the pyrolysis unit and the hot catalyst is circulated to provide heat for the pyrolysis stage. The total solid circulation in pyrolysis reactor is a combination of feed plus catalyst flow rate and in the combustion chamber only refers to the catalyst. The catalyst

inventory undergoes a daily replenishment of 3% to account for losses and attrition. The *in situ* CFP configuration combines polymer thermal deconstruction and the catalytic upgrading of pyrolysis vapors in the same reactor as opposed to upgrading in a different reactor (*ex situ* CFP).

Besides catalyst composition and residence time, the catalyst-to-feedstock (C/F) ratio is a primary contributor to product selectivity in plastics CFP.[67,68] In the four case studies, which all use the same substrate feed rate, we varied the C/F ratio from 4–28 to model the desired products (Table 1). Previous work has shown that a high C/F ratio facilitates the production of light olefins, whereas a lower C/F ratio favors the production of aromatic products.[32,55,56] After the pyrolysis reactor, rapid quenching of the pyrolysis effluent generates liquid (C_5–C_{20} hydrocarbons) and gaseous products (C_1–C_4 hydrocarbons), and solid char. Product recovery is modeled using conventional refinery operations.[69–71] Table 1 lists the product compositions and other operating assumptions for all cases.

In all cases, the MSP of the primary product was estimated by evaluating discounted cash flow with a 10% internal rate of return (IRR) factor over a 30 year plant lifetime, such that the net present value (NPV) is zero. The major financial parameters used in the discounted cash flow analysis are listed in Table S2 (ESI†). Sales of different co-products contribute to the revenue in estimating the MSP of the primary product – *i.e.*, naphtha (Case A), BTX (Cases B and C), and ethylene (Case D). The designation of the primary product was based on the expected highest revenue (combination of its yield and average price), while the remaining products are designated as co-products.

We employed the MFI tool to estimate the total supply chain energy and GHG emissions for the four cases based on the material and energy balance data from the Aspen Plus models.[72] The life cycle impacts were determined using SimaPro LCA software and ecoinvent version 3.3 background data (allocation, cut-off by classification – unit, United States-specific inventories when available, global inventories otherwise).[73] Additionally, the economic and sustainability metrics were compared to the conventional petroleum manufacturing route.[20] Establishing the appropriate conventional baseline is complicated by the fact that the pyrolysis process cases considered yield multiple products. Rather than perform an allocation (mass-based or otherwise) for only one of the products of interest, all products are included, and the corresponding conventional baseline is taken to be a normalized proportional average of impacts from each of the constituent petroleum parts of the product stream (from each of their respective petroleum routes), as described below.

TEA results for Case A – naphtha product

Fig. 2a presents a simplified process flow diagram for Case A. For the production of naphtha from CFP, we modeled an *in situ* CFP reactor at 550 °C and 1 bar, with a 2 s residence time. A mix of spent FCC catalyst and ZSM-5 produces a naphtha stream (C_5–C_{12} hydrocarbons), of which aromatics comprised 76 wt% (Table 1).[54] Other products, such as char and heavier hydrocarbons, containing predominantly waxes (C_{24} +, boiling points >370 °C) and diesel-range (C_{12}–C_{20}, boiling points ~220 °C–370 °C) compounds, are used as process fuel within the waste plastic processing facility. The gaseous fraction (~46 wt%), which contains light alkanes, olefins, CO_2, CO, H_2, and CH_4, is recycled back to the pyrolysis reactor to assist fluidization (Fig. 2a).

The total capital investment for a 240 TPD naphtha production facility was estimated at $77.6 million (Fig. 2b and Table S3, ESI†) with a yearly operating expense of about $65 million (Fig. 2c). Since some of the major equipment costs were derived from estimations based on similar equipment,[57] or from costs derived from mechanical design tools, we included sensitivity analysis to show the impacts of changes in capital cost assumptions in the next section (Case B). The MSP of the naphtha stream is $2.18/kg (Fig. 2d), which is 4-fold that of average petroleum-derived naphtha ($0.50/kg) over a period of 5 years (2016–2020).[74]

TEA results for Case B – mixed product

The process flow diagram for Case B, which is also the base case, is shown in Fig. 3. In this case, the pre-processed mixed plastic waste is modeled to be fed to the pyrolysis reactor and reacted at 670 °C and 3 bar with a residence time of 2 s. The effluent products are then cooled to yield 47 wt% gas and 50 wt% liquid products.[54] Herein, olefins constitute ~35 wt% of the gases, and aromatics constitute ~33 wt% of the liquids (of which the BTX mixture is ~22 wt%).[74] Details about the process design can be found in the *Materials and Methods* in the ESI,† including detailed process flow diagrams for each process section (Fig. S1–S4, ESI†) and product yields are shown in Table 1.

Capital expenses. The total capital investment (TCI) for a plant designed to process 240 TPD of mixed plastic waste in Case B was estimated to be $107 million (Fig. 4a and Table S4, ESI†). The total direct costs associated with each process section, which includes a total installed capital (TIC) cost of $55.8 million, are estimated to be around $64 million, while the indirect costs for project planning and construction are estimated to be around $38 million. The remaining $5 million is for land and working capital expenses. The CFP area accounts for the largest inside battery-limit investment due to the pyrolysis reactor and the coupled combustion-regenerator system, compressors for flue gases, cyclones, and coolers. Furthermore, light olefins – which are recovered at very low temperatures (−20 °C to −103 °C) and high pressure (up to 37 bar) – account for $10 million, or roughly 20% of the total equipment costs. Additionally, a 25% contribution is assumed from the outside battery limit investment, which consists of additional capital expenditure (*e.g.*, development of piping, instrumentation *etc.*) required to integrate the over-the-fence utilities into the plant. Detailed information on the specific unit operations and the capital requirements for each process section is provided in Table S4-S6 (ESI†). Overall, capital recovery charge, which includes capital depreciation (capital costs), annual income tax, and return on investment,

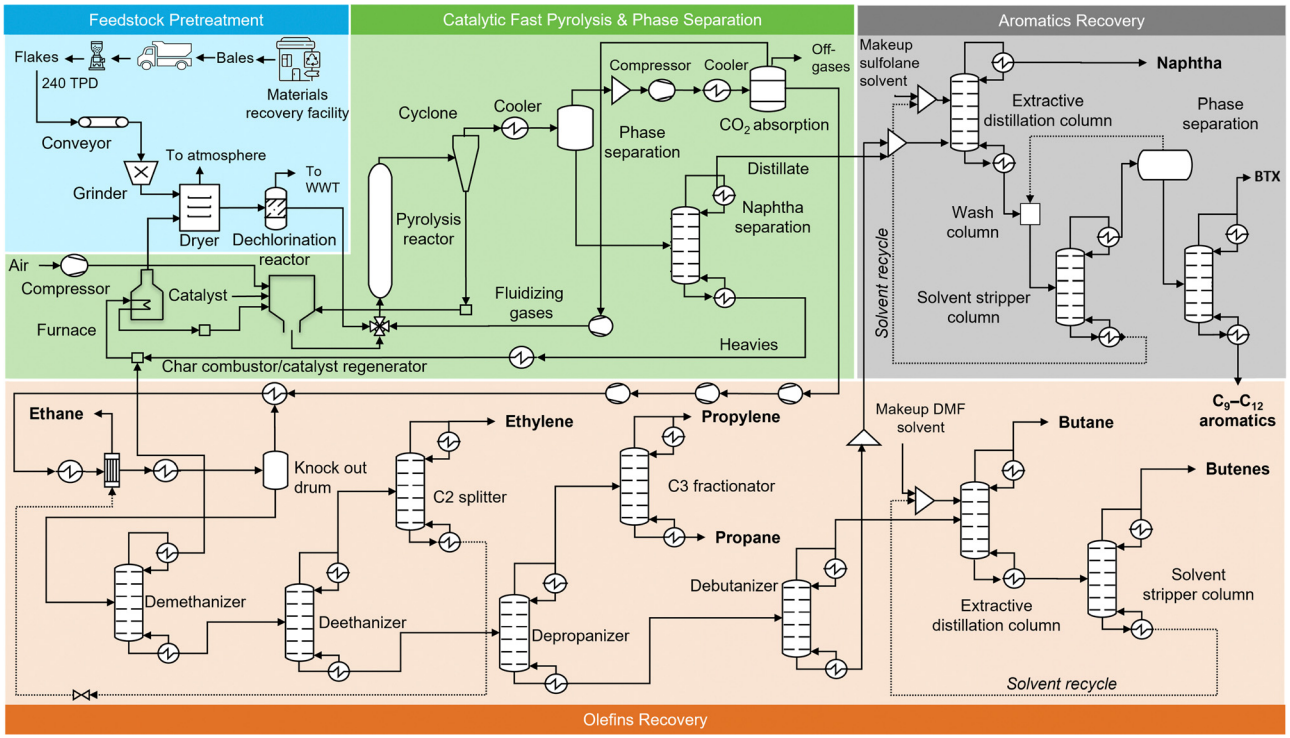

Fig. 3 Process flow diagram of a waste plastic refinery based on CFP. Feedstock Pretreatment: This section includes plastic flake production equipment, conveyor belts, grinder (~2–3 mm), a dryer, and a PVC removal reactor. Catalytic Fast Pyrolysis (CFP): The CFP area uses an *in situ* dual-stage circulating fluidized bed reactor[57] to convert mixed plastic waste into hydrocarbon vapors, which are subsequently cooled to produce a gaseous stream and a liquid stream. Char and catalyst are separated from the vapors *via* cyclones, and the heat for the pyrolysis reaction is generated by the combustion of process char and heavy hydrocarbon fraction (C_{24}+ hydrocarbon) in a combustor. Phase separation: The hot pyrolysis effluent is cooled to obtain an olefins rich gaseous stream and an aromatics-rich liquid stream. Olefins recovery: The CO_2 is first removed from the olefins-rich vapor stream, after which it enters a chilling train. Hydrogen and methane are removed through a demethanizer column, and ethylene and ethane are further removed in a C2 fractionator, after the deethanizer column. Propylene and propane are separated from the C4 mixture *via* a depropanizer and are further recovered as pure streams in a C3 splitter. C_4 hydrocarbons are removed in a debutanizer and are further separated into butane and 1-butene streams through an extractive distillation process. The bottom of debutanizer (C_5+ hydrocarbon) moves to the aromatic hydrocarbons recovery area. Aromatics recovery: Finally, the liquid stream from the olefin recovery area and CFP and phase separation area is introduced into an extractive distillation column to recover BTX aromatic hydrocarbons using sulfolane as the solvent. The process also produces naphtha and C_9–C_{12} aromatics. The detailed process flow diagrams with labeled streams and a corresponding table of stream compositions of each process sections are included in Fig. S1–S4 (ESI†).

contributes \$0.87/kg to the MSP of BTX aromatic hydrocarbon product (Fig. 4c).

Operating expenses and revenue from co-products. In addition to the total capital investment, the plant requires operating expenses of \$84 million per year. These expenses include feedstock cost at \$52 million per year (mixed waste plastics were purchased at \$0.18/kg and converted to flakes at an additional \$0.42/kg), and the expenses for the process utilities, which amount to \$23 million per year, include the cost of sulfolane solvent for BTX extraction, which is estimated at \$10 million per year as indicated in Fig. 4b. Other costs for the feedstock pre-treatment process section (Fig. 4b) include operating expenses for a washer, dryer, and hammermill, as well as installed equipment costs. The pretreatment contribution for the base case is included in Table S4 in the ESI.† Fixed operating costs, which amount to approximately \$9 million, include labor and overhead costs. Integration of the heating and cooling utilities lowers the overall energy requirement of the process. Particularly, the use of char and heavy hydrocarbons for combustion provide the necessary heat to the pyrolysis reactor. Annual revenue from the sale of multiple co-products (olefins and aromatics) is \$82 million, which offsets the overall annual expenses (Fig. 4b and Fig. S5, ESI†). Table S7 (ESI†) contains a detailed breakdown of the contribution of different process sections to the annual operating expense in Case B – mixed product.

MSP of BTX product

Fig. 4c shows the TEA results for Case B. The MSP of the key product, namely the BTX aromatic hydrocarbons mixture, is \$1.07/kg, which is approximately 1.6-fold higher than the average price of petroleum-derived BTX (\$0.68/kg) over a period of 5 years (2016–2020).[74] The high cost of BTX production (approximately \$6.0/kg, without the sale of co-products) is reduced by the recovery and sale of co-products (Fig. 4d). Table S8 (ESI†) reports the average market prices of product and co-products obtained in Case B and basis of their pricing.[74] A summary of the process and economic results for Case B is provided in Table S9 (ESI†). We investigate Case B in more

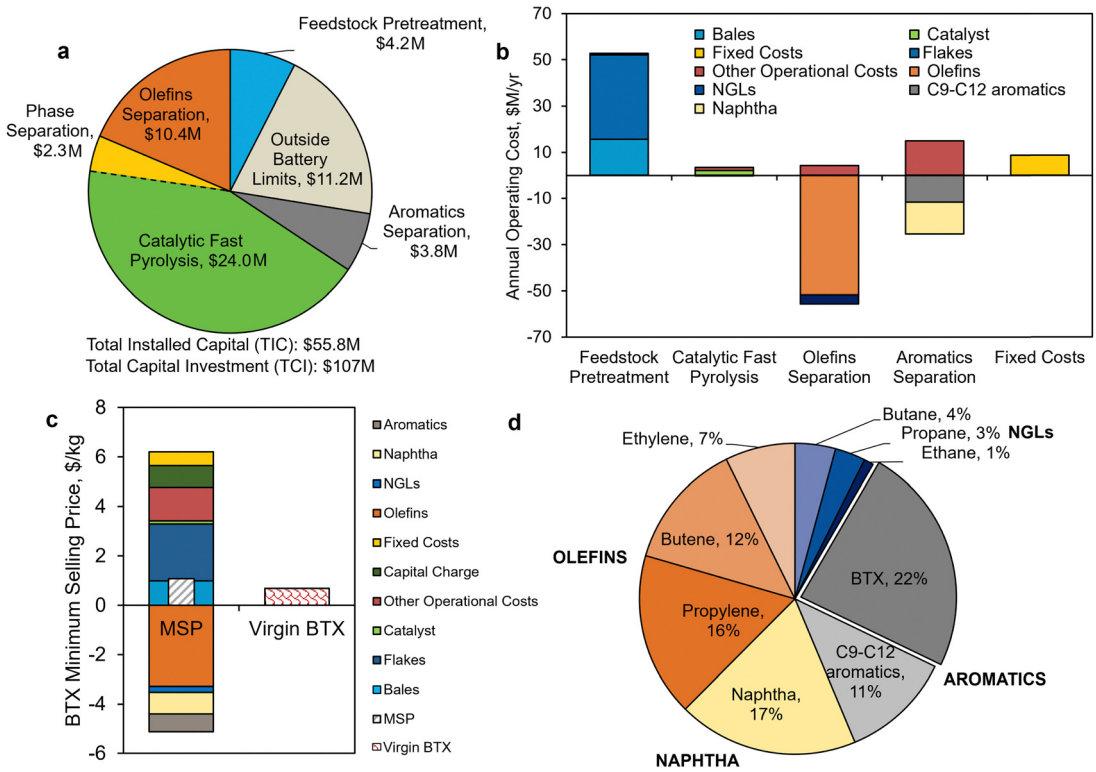

Fig. 4 TEA results of Case B – mixed product. (a) Capital cost breakdown by area for each process section, with total installed capital (TIC) of $55.8 million and total capital investment of $107 million. (b) Annual operating expenses for the base case, disaggregated by process step (total = $84 million per year). The highest contribution is from feedstock costs. Fixed costs include labor and overhead. Note that BTX is not considered a co-product in estimating the annual operating expenses. (c) The minimum selling price (MSP) breakdown of BTX aromatics relative to virgin BTX manufacturing. (d) The contribution of co-products towards the MSP. Aromatics streams comprise BTX and C_9–C_{12} aromatics. Natural gas liquids (NGLs) consist of ethane, propane, and butane. All data shown in Fig. 4 are included in Tables S4–S6 (ESI†) for Fig. 4a, Table S7–S12 (ESI†) for Fig. 4b and Tables S13, S14 (ESI†) for Fig. 4c.

detail here as it serves as a basis for Case C – aromatics-rich product and Case D – olefins-rich product.

Sensitivity analysis. A univariate sensitivity analysis was conducted to identify the parameters that exhibit substantial impacts on the economic feasibility of plastics CFP. Fig. 5a shows a tornado chart summarizing the magnitude of impacts from key process variables on the MSP of the BTX product. As shown in Fig. 5a, increasing the feedstock cost from $0.60/kg (baseline) to $0.70/kg increases the MSP by 51%. Conversely, pyrolysis could be below cost parity at a feedstock cost of $0.50/kg. Overall, there is a linear relationship between feedstock price and MSP, implying that the economic feasibility of plastics pyrolysis is highly sensitive to the feedstock price (Fig. 5b). Fig. S6 (ESI†) depicts a sensitivity analysis designed to specifically capture the effects of fluctuating costs of flakes, a key component of the total feedstock cost that significantly impacts the economic viability of the project.

Next, we evaluated the potential for integrating pyrolysis intermediate streams with a traditional petroleum refinery through the ''Downstream Capital'' sensitivity parameter. Product separations account for ~25% of the total installed capital ($14 out of $56 million, Fig. 4a), given the base case assumes a greenfield plant. In the case where the intermediates can be recovered in an existing petrochemical refinery, which is denoted ''0'' in Fig. 5a on ''Downstream Capital'', it is assumed that no capital investment will be required for product separations. For this scenario, the base case MSP is estimated to decrease 32% to $0.73/kg.

Additional variables were also examined in this sensitivity analysis. Notably, increasing the IRR to 15% (baseline IRR 10%) increased the MSP by 30%. We varied the variable operating cost (excludes the feedstock, waste disposal costs and fixed costs) by ±5M dollar per year (equivalent to ±22% of the base case cost of $23 million), especially given the uncertainty of sulfolane price (the solvent for BTX aromatic hydrocarbons recovery). The sensitivity analysis shows, unsurprisingly, this to be a major cost driver. The impact of plant size on the MSP was evaluated considering no additional process or feedstock differences, demonstrating that the MSP can be reduced by 14% due to economies of scale when the plant size is doubled (500 TPD) from the base case. Finally, the tornado plot also shows that a higher downtime (86% plant on-stream factor *versus* 90% in the base case) results in an increase of 7% in the BTX MSP. Additional sensitivity parameters such as income tax rate and working capital were not found to have a substantial impact.

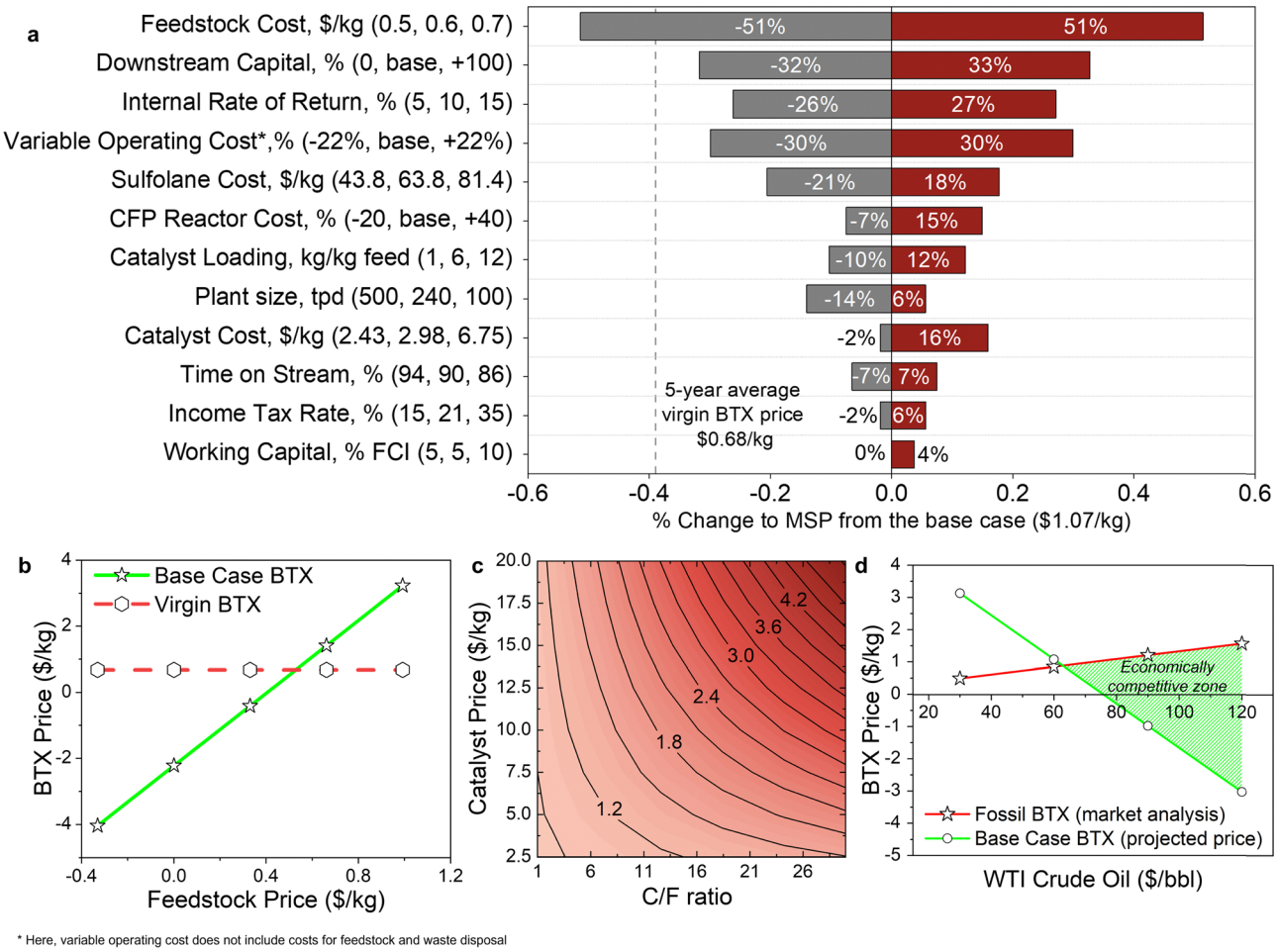

* Here, variable operating cost does not include costs for feedstock and waste disposal

Fig. 5 Sensitivity analysis of the Case B – mixed product. (a) Results of single-point sensitivity analyses for relative change to process and financial variables on the MSP of BTX aromatics (price = $1.07/kg). For each sensitivity case, the variable was modified to a high and a low value, while holding all other variables constant to the base case. The minimum and maximum values used in this analysis are shown in the vertical axis labels as low (gray): base: high (red). The central line represents the base case prices. The basis for selecting the lower bound and higher bound values of the univariate sensitivity parameters is presented in Table S15 (ESI†). The base case downstream capital cost, variable operating cost, CFP reactor cost, and plant size values are $14.2 million, $25.8 million, $14 million, and 240 TPD, respectively. (b) MSP of BTX aromatics as a function of plastic feedstock cost. (c) Multivariate sensitivity analysis for the effect of change of catalyst cost and loading on MSP of BTX aromatic hydrocarbons. Base case values for C/F ratio and catalyst cost were 6 and $2.98/kg, respectively. (d) Illustration of profitability scenario of the BTX product as a function of West Texas Intermediate (WTI) crude oil price in $ per barrel ($/bbl). Data shown in Fig. 5a are included in numerical form in Table S16 (ESI†).

A multivariate sensitivity analysis was also conducted (Fig. 5c) to assess the impact of C/F ratio as a function of catalyst cost on the MSP of main product. Increasing the catalyst loading (C/F = 18) and the catalyst cost to $12.5/kg was found to increase the estimated MSP by more than 55%. Further, to capture the variations in crude oil and petroleum product prices, a sensitivity analysis on the product prices as a function of a benchmark crude oil price was conducted by employing a simplified pricing structure adopted and modified from Talmadge *et al.*[75] Data from the Oil Price Information Service (OPIS) International Feedstocks Intelligence Reports for WTI—one of the crude oils was used as a benchmark in oil pricing—ranges from $30–$120/bbl; the prices of the specific year served as the basis for the analysis product pricing structure. To capture the product pricing basis comprehensively, additional sources were included mainly S&P Global PLATTS, US Energy Information Administration (EIA) and IHS Markit. Fig. S7 and S8 (ESI†) shows the pricing equations and the trend of the price change in the product and co-products with a benchmark crude oil price.[75] When benchmark crude oil (West Texas Intermediate, WTI) is $30/barrel, the market prices for all fossil-derived co-products is low, implying that the BTX MSP will be almost 3-fold higher (Fig. 5d). However, if the price of WTI crude oil increases to $100/barrel, causing an increase in the prices of petrochemical products, the base case BTX aromatic hydrocarbons MSP will drop, while the price of fossil-derived BTX mixture will increase. Thus, the WTI crude oil price has a significant impact on the profitability of the CFP refinery, with co-product pricing serving as the main factor in generating high revenues.

TEA results for Case C – aromatics-rich product

This scenario converts plastic feedstock into an aromatics-rich naphtha-range hydrocarbon stream (69 wt%), which has

approximately 2-fold higher aromatics content (60%) than the Case B – mixed product (Table 1). The aromatics-rich naphtha (69 wt%) is separated downstream to recover the BTX aromatic hydrocarbons by an extractive distillation process identical to that described in Case B. Other co-products such as olefin monomers are also recovered, albeit in smaller quantity (olefins at 16 wt% and NGLs at ~10 wt%) because of the trade-off in the carbon distribution between olefins and aromatic hydrocarbons.[34] The main difference is in the use of a zeolite catalyst with a comparatively higher Si/Al ratio (lower acidity) than Case D and residence time/pyrolysis conditions employing a higher heating rate (>600 °C s^{-1} compared to Case B of ~500 °C s^{-1}).[55,56] Higher aromatic hydrocarbons productivity due to catalyst choice and amount in the *in situ* reactor formed the basis of this scenario, assuming all other parameters remain the same.

The MSP of BTX aromatic hydrocarbons in Case C is \$0.95/kg, which is 11% less than the MSP of \$1.07/kg of BTX product in Case B and is only 1.4 times fossil-derived BTX aromatic product (Fig. 6a). The operating and capital costs along with the comprehensive economic summary of Case C is provided in Table S17 (ESI†).

TEA results for Case D – olefins-rich product

Here, we modeled a higher yield (64 wt%) of low-molecular-weight olefins (such as ethylene, propylene, and butene) than the Case B olefins (35 wt% olefins) (Table 1). A catalyst with larger pore diameter and low Si/Al ratio (higher acid content per mass catalyst than that used in Case B and C) and a high C/F ratio of 28 with a shorter residence time (1–2 s) was modeled in the pyrolysis reactor, which can result in increased cracking of the plastic feedstock, resulting in higher yields of gaseous olefins.[55,56,76]

Compared to the petroleum-derived route for ethylene production, the MSP of ethylene from mixed plastic waste pyrolysis is \$0.85/kg (1.4 times fossil-derived ethylene price at \$0.61/kg) (Fig. 6a). The operating and capital costs and economic summary of Case D are provided in Table S18 (ESI†).

Supply chain energy and GHG emissions

The supply chain energy consumption (MJ $kg_{product}^{-1}$) and GHG emissions (kg CO_2-eq per $kg_{product}$) were evaluated using the MFI tool for the four cases (Fig. 6b and c). The mass and energy stream flows from the Aspen Plus process models were used as process inventory inputs to MFI. Supply chain energy accounts for all energy inputs into the process, including process fuel for heating, electricity, transportation energy, and energy contained in fossil-derived chemical feedstock. GHG emissions are the sum of combustion processes within the supply chain, mainly process heating, electricity generation, and transportation of inputs; emissions arising from chemical reaction stoichiometry are not included in the scope of MFI.[77] Both of these metrics are normalized to the functional unit of 1 kg of product.

Compared to fossil-derived naphtha, Case A – naphtha product is estimated to exhibit a 45% reduction in supply chain energy usage, but a 2-fold increase in GHG emissions. In the case of the incumbent process for naphtha production, feedstock is the major contributor to supply chain energy. Because there is no associated burden with the use of mixed plastic waste feedstock, which is considered "waste", supply chain energy is significantly reduced in Case A. In contrast, the increase in GHG emission is due to the higher use of process utilities, such as electricity and fuel in Case A. There is also a major fraction attributed to feedstock pretreatment that includes feedstock collection, sorting at a MRF, processing into

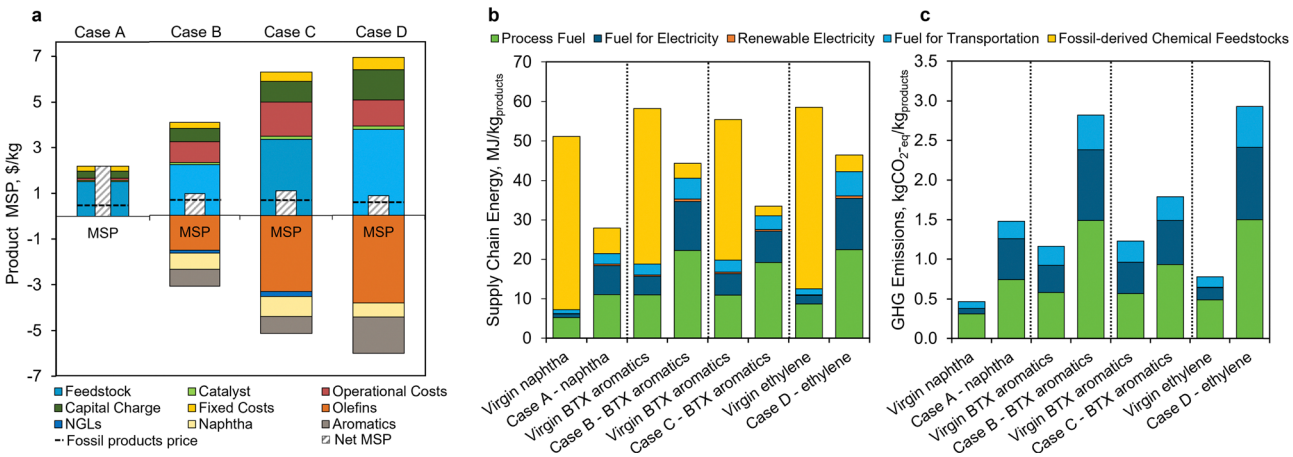

Fig. 6 Comparative summary of the economic and environmental analysis of the different pyrolysis scenarios proposed in this study. (a) Economic summary: Case A shows the MSP breakdown of naphtha product as a function of process variables, Case B shows the MSP breakdown for BTX aromatic hydrocarbons. The MSP of \$1.07/kg is 1.6 times higher than virgin BTX aromatic hydrocarbons (\$0.68/kg). Case C – aromatics-ich product has BTX aromatic hydrocarbons as the main product and is estimated at an MSP of \$0.95/kg. Finally, Case D – olefins-rich product with ethylene as the main product is estimated at an MSP of \$0.85/kg, which is 1.4 times that of virgin ethylene (\$0.61/kg). Note that dotted lines show the price of fossil-derived products for the respective cases. (b) Supply chain energy and (c) GHG emissions of the four cases relative to virgin manufacturing. Fig. S9 (ESI†) illustrates a comparison of GHG emissions calculated by MFI *versus* LCA. Fig. S10 (ESI†) shows the system boundaries for the MFI analysis. All supply chain energy and GHG emissions data are in Tables S19–S22 (ESI†).

flake, and transportation to the pyrolysis facility. These supply chain energy and GHG emission values could change substantially with alternate process configuration (*in situ vs. ex situ*) resulting in improved process yields (due to less challenging environment for the *ex situ* catalyst) as well as through additional process heat/energy integration and product downstream separation.[44,45,57]

Furthermore, the BTX aromatic hydrocarbons produced from Case B is estimated to have 24% lower supply chain energy requirements and 2.4 times higher GHG emissions compared to the fossil-derived BTX production pathway. The estimated GHG emissions are 2.82 kg CO_2-eq per kg_{BTX} in Case B, whereas fossil-derived BTX mixture emits 1.16 kg CO_2-eq per kg_{BTX}. Unlike Case A, significant (negative impact) contribution from co-products lowers the overall energy and GHG emissions. In Case C – aromatics-rich product, the total supply chain energy and GHG emissions show a 40% reduction and 46% increase, respectively, relative to the fossil-derived counterpart. These energy requirements and GHG emissions are linked to process yields, and thus a greater yield of more beneficial products reduces the associated environmental impacts by using fewer utilities and resources per unit of product. Finally, the total supply chain energy in Case D is estimated to exhibit a 21% reduction, with a GHG emissions increase of 3.8 times. The higher GHG emissions are due to the use of more energy-intensive process utilities for separation of olefins that occurs at high pressure and low temperature conditions, as well as a lower yield of the ethylene product per unit of incoming plastic feedstock. As explained above, the lower supply chain energies exhibited by all four cases are primarily due to the use of mixed plastics feedstock in the pyrolysis facility. As shown in Fig. 6b (yellow portion), the fossil-derived chemical feedstock is the largest contributor to supply chain energy, but it is almost absent from the mixed plastic waste process scenarios.

Life cycle assessment

While MFI provides detailed insight into GHG emissions and energy consumption within the current U.S. supply chain, LCA offers a more holistic overview of environmental impacts from a global perspective. We used the Tool for the Reduction and Assessment of Chemicals and Other Environmental Impacts (TRACI 2.1, US 2008)[78] and Available WAter REmaining (AWARE)[79] methods and ecoinvent version 3.3 background data (U.S.-specific when available, global otherwise)[73] in SimaPro LCA software to calculate the acidification, carcinogenic toxicity, ecotoxicity, eutrophication, fossil fuel depletion, non-carcinogenic toxicity, ozone depletion, particulates formation, smog, and water use impacts of pyrolysis of mixed plastic waste to various products (Fig. 7 and Table S23–S26, ESI†). The process was assessed using a cradle-to-gate approach, where the ''cradle'' is collection of mixed recyclables from curbside bins and the ''gate'' is the output(s) of the pyrolysis plant. Manufacture of the original plastic feedstock and utilization of the produced chemicals are not included. The inventory was developed based on the reported Aspen Plus process model and data from the literature for collection and sorting.[80] Credits were given for co-products, wherever applicable. Standard deviations were estimated using ecoinvent uncertainty distributions and Monte Carlo analysis with 1000 iterations.

Case A for naphtha production exhibits lower fossil fuel depletion and ozone depletion than fossil-derived naphtha on a statistically significant basis, but higher acidification, ecotoxicity, eutrophication, global warming, carcinogenics, non-carcinogenics, particulate formation, smog, and water use (Fig. 7a and Table S23, ESI†). Most of these impacts are associated with collection, sorting, flaking and transportation of the plastic feedstock (53–96% of all metrics except water use), electricity (6–25%), steam (1–9%), and methane (1–21%, Fig. 7b). The global warming potentials reported by LCA are generally higher than those observed in MFI due to the inclusion of process emissions (0.88 kg CO_2-eq per $kg_{naphtha}$, 1.85 kg CO_2-eq per kg_{BTX}, 1.23 kg CO_2-eq per kg_{BTX}, and 1.40 kg CO_2-eq per $kg_{ethylene}$ for Cases A, B, C, and D, respectively, see Tables S23–S26, ESI†) and different background data assumptions (U.S. *versus* global), but the comparative trends between virgin production and pyrolysis remain similar. Fig. S9 (ESI†) compares the MFI and LCA results for GHG emissions and provides further commentary. The values for fossil fuel depletion in LCA and supply chain energy use in MFI are not directly comparable as supply chain energy use is reminiscent of embodied energy at a single time point, whereas fossil fuel depletion incorporates a weighting factor that adjusts the impact of a given energy input based on the potential for that fuel to become more difficult to extract in the future.[81]

Case B for BTX aromatic hydrocarbons production has lower fossil fuel depletion and ozone depletion than fossil-based BTX, with the remaining life cycle categories demonstrating impacts 1.2 to 76 times higher (Fig. 7c and Table S24, ESI†). All these results excepting acidification, carcinogenics, smog formation, and water use are on a statistically significant basis. Plastic feedstock, refrigeration, steam, and electricity account for 32–82%, 12–48%, 2–25%, and 4–13%, respectively, of all metrics except water use, which is dominated by cooling water (Fig. 7d). Further heat integration in the olefins and aromatics separation areas, which is already implemented in the process models to a certain extent, will be crucial for minimizing utilities. Using a catalyst for high aromatic selectivity (Case C) presents an opportunity to improve the environmental impacts of pyrolysis-derived BTX aromatic mixture: acidification, fossil fuel depletion, ozone depletion, and smog formation become lower than virgin BTX in this scenario (Fig. 7e and Table S25, ESI†). This is due to enhanced BTX aromatic hydrocarbons production and a corresponding reduction in utilities and consumables (particularly plastic feedstock) required per unit product, as well as an increase in naphtha and C_9–C_{12} aromatic co-products, which provide larger environmental credits across most categories than olefins or paraffins (Fig. 7f).

Lastly, ethylene production in the olefin-rich scenario (Case D) is predicted to exhibit lower fossil fuel depletion on a statistically significant basis, but all other categories are higher than virgin ethylene by 2 to 1700 times (Fig. 7g and Table S26, ESI†). These impacts are primarily associated with consumables such as plastic feedstock (29–80% of all metrics

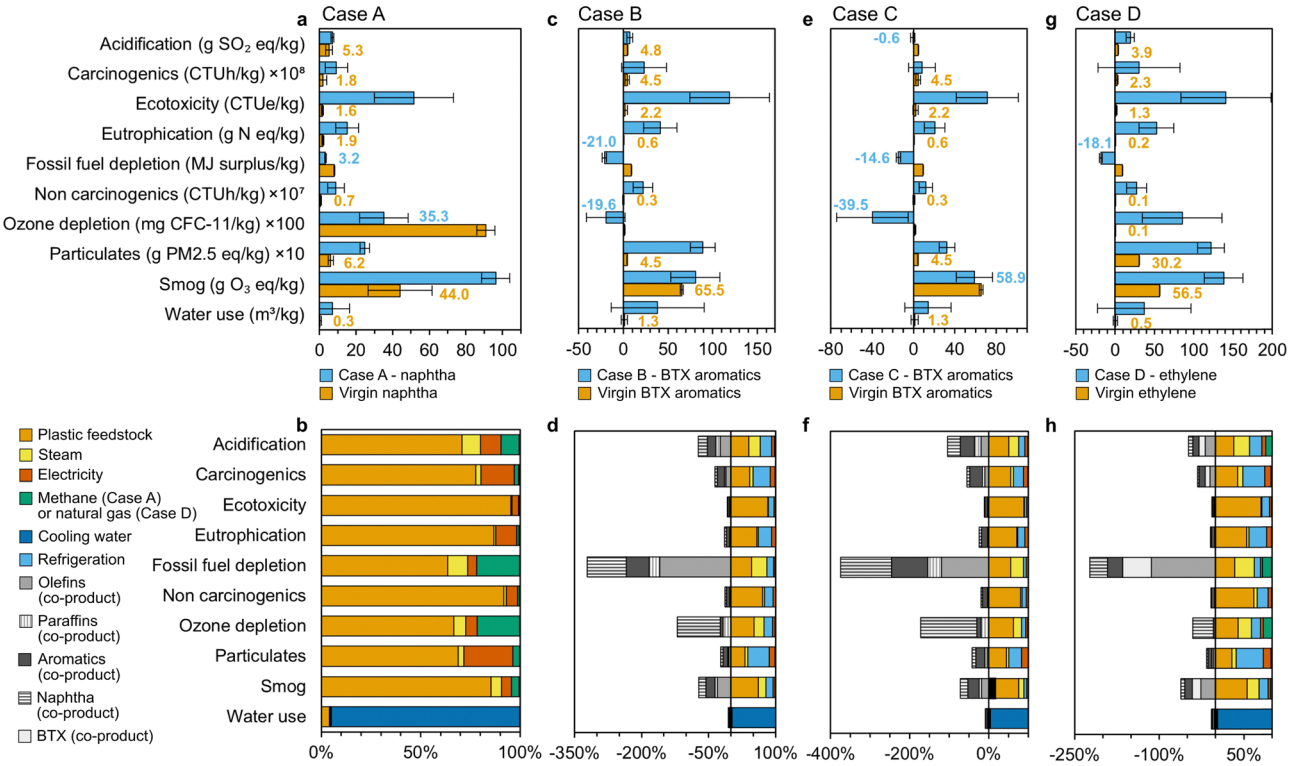

Fig. 7 Life cycle assessment for pyrolysis of mixed plastic waste to naphtha, BTX aromatic mixtures and ethylene under different process scenarios. (a) Comparison of the Case A – naphtha product to virgin naphtha, (b) contributions of various process components to the overall environmental impacts of the Case A. (c) Comparison of the Case B – mixed product (where principal product is BTX aromatic hydrocarbons) to virgin BTX mixture, (d) contributions of various process components to the overall environmental impacts of the Case B. (e) Comparison of the Case C – BTX aromatics rich product to virgin BTX aromatic mixture, (f) contributions of various process components to the overall environmental impacts of the Case C, (g) comparison of the Case D – ethylene monomer product to virgin ethylene, (h) Contributions of various process components to the overall environmental impacts of the Case D. Aromatic co-products include C_9–C_{12} aromatics, paraffin co-products include ethane, propane, and butane, and olefin co-products include ethylene, propylene, and butene. Components with contributions less than 1% (catalyst, process water, dimethylformamide (DMF) solvent, infrastructure, and wastewater treatment) are not included in the figure. Calculations were conducted with TRACI 2.1 US 2008 and AWARE methods, SimaPro software, and ecoinvent 3.3 background data. All data shown in Fig. 7a–h are included in numerical form in Tables S23–S26 (ESI†).

except water use), refrigeration (12–48%), steam (2–34%), electricity (3–13%), and natural gas (0.3–16%), which are higher per unit product because less ethylene (1778 kg h^{-1}) is produced than naphtha (4350 kg h^{-1}) or BTX (2008–2,991 kg h^{-1}) in the previous cases and the olefin recovery stage is energy intensive (Fig. 7h). Fewer environmental credits are also received from propylene and butene in comparison to naphtha, BTX, and C_9–C_{12} aromatic compounds.

Discussion

In this study, we identified drivers of economic and environmental impacts for four different scenarios describing a plastic waste pyrolysis facility. Several aspects are considered here that are relevant to both the process economics and environmental feasibility.

Feedstock cost and quality

The U.S. national average market prices for reclaimed post-consumer plastics in 2019 varied widely between \$0.03–\$0.70/kg,[60,61] depending on the material demand, purity, color, format, and processing cost. Plastics for which sorting is not conducted – *e.g.*, 3–7 resin identification code, including flats, films, and flexibles – usually are landfilled.[61,82] Sourcing plastics that are routinely landfilled may enable lower feedstock cost, which is the primary economic driver reported here (Fig. 4) and in previous studies.[46,47] Pyrolysis may be an option for valorizing mixed plastics, given its potential ability to tolerate contamination,[83,84] but the use of pyrolysis oil (naphtha) directly as feed to the steam cracker may be limited by impurities.[4] Few studies to date have systematically evaluated the effect of feedstock composition or the presence of contaminants on CFP process viability.[85,86] A plastic composition rich in polyolefins is most desirable for the production of fuels and petrochemicals. The presence of PET, PS, and PVC reduces the overall yield of the pyrolysis process and produce undesirable products such as styrene, gaseous components and acidic species.[66,87,88] The chemical components of plastic waste-derived pyrolysis oils should be carefully considered prior to use as fuels or chemical feedstocks.[38,89]

Determination of plant size

The size of a pyrolysis plant will likely depend on the waste processing capacity of regional MRFs. Additionally, the

transportation distance between MRFs and pyrolysis facility can also influence the plant size, which in turn can impact financial viability and environmental impacts. For example, Larrain *et al.*[90] estimated that the minimum throughout of a waste plastic pyrolysis plant must be about 250 TPD to achieve an IRR of at least 15%. This is in agreement with our findings because the capital and operational investments can greatly exceed the revenues (and heat integration becomes challenging) for a pyrolysis plant operating at a smaller scale (<50 TPD).[46,48] At present, commercial operations from pilot scale to commercial scale are in the range of 10 tpd to 300 tpd.[62,91,92] Sensitivity analysis shows that increasing the plant size to 500 TPD leads to a 14% reduction in MSP of the BTX product, but collection and logistics would need to be optimized to provide a reliable supply of waste plastics.[93]

Catalyst design

One of the most direct strategies to increase the economic and environmental benefits of a plastic waste CFP refinery is to increase the selectivity to desirable products. Improving process selectivity will enable the production of higher yields of valuable products from the same quantity of feedstock, which is the largest process operating expense in this study. Selectivity can be controlled through catalyst choice. Zeolites in particular have been widely used to increase selectivity to olefins and aromatic compounds.[4,94] In the cases described above, catalysts from the petroleum processing industry were examined. However, work is underway to develop catalysts specialized for waste plastic CFP processes.[95] Several works have demonstrated how control over pore size and topology,[96] the addition of transition metals,[97] and changes in catalyst acidity can be used to increase the yield of aromatics and light olefins from waste plastic catalytic pyrolysis.[98] The value of these improvements is underscored in Fig. 6, where an increase in BTX aromatic hydrocarbons yield between Case B (revenues $15.5 million per year) and Case C (revenues $24 million per year) decreases the primary product MSP by 11.2%.

Carbon efficiency of plastics pyrolysis

In our study, we relied on literature to model a plant that results in complete conversion of mixed waste plastic and with >90% product recovery.[57,69] Due to a short residence time (<2 s), yields of solid char (3 wt%), methane, and secondary cracking products were minimized.[69] Our catalyst selection of spent FCC catalyst with ZSM-5 transforms mixed waste plastics into C_2–C_4 olefins (~34 wt%) and BTX aromatic hydrocarbons (~20 wt%), with negligible C_{24}^+ products (~1 wt%).[54] Moreover, the CFP catalysts are regenerated and re-used in plastic pyrolysis facility with only a 3% loss, which is much better than disposal in landfills. Our strategy also overcomes some of the concerns of using fresh FCC catalysts, such as the loss of carbon to coke or methane, avoids disposal concerns of the used catalyst to landfills, impacting sustainability metrics.[32,67,99] Overall, because of the inherently high carbon content of waste plastics and through catalyst design, pyrolysis processes show a higher conversion of carbon into useful products compared to similar biomass or municipal solid waste pyrolysis.[100,101]

Refinery integration of pyrolysis-derived intermediates

Plastics pyrolysis produces a range of products, which necessitates downstream separations that can account for the second-highest contribution to the MSP (Fig. 4). Moreover, the market shift from fuel production towards plastics and petrochemicals manufacturing offers a potential opportunity for co-processing plastics-derived pyrolysis oils in existing refinery infrastructure, which can potentially reduce capital expenses to build cracker units.[4,102,103] Additionally, diverting to steam cracking can provide an example of closed-loop recycling for olefin monomers. However, as mentioned, the presence of contaminants in the co-mingled waste plastics may result in a low-quality pyrolysis naphtha, which may need to be decontaminated to obtain a high-quality feedstock.[4,7,104] Furthermore, the heat-transfer rate has to be optimized with an increase of reactor size, posing a scale-up challenge associated with feedstock anisotropy and equipment sizing.[105] Future R&D activities should establish the technical risks associated with catalyst deactivation, including its impact on catalyst lifetimes and replacement rates, as well as the risks of introducing contaminants into refineries.

Profitability measures

The TEA in the current study was focused on projecting the MSP of the primary product from Cases A–D. We estimate the initial capital investment for the construction of a pyrolysis facility and annual operating expenses required for processing mixed plastics waste. In our case, with multiple (N) products being produced, we estimate the revenue from the sale of other (N-1) products and compute the MSP of a primary product such that the NPV is zero. However, the selection or designation of a primary product is somewhat a subjective choice mainly based on the expected highest revenue. Alternatively, several other metrics such as NPV (with the average market prices for sale of all products), IRR, return on investment, and energy return on investment may be alternatively used to assess the economic feasibility; however, we stress that the use of these alternative metrics would not the change the overall conclusions of the study.

Environmental impacts

As shown in Fig. 6b, the utilization of fossil feedstocks (such as natural gas and crude oil) accounts for the bulk of supply chain energy consumption for the production of conventional C_2–C_4 olefins and BTX aromatic compounds.[106,107] Conversion of plastic waste *via* pyrolysis to produce the same products directly eliminates a large portion of the supply chain feedstock and energy needs, making the entire waste plastic processing process less energy intensive than the conventional fossil-derived process. In addition to fossil feedstock energy, other supply chain energy types such as process fuel (steam, cooling water), electricity, and transportation fuel contribute to overall energy impacts and must be considered to understand the

implications of adopting pyrolysis. Overall, the supply chain energy consumption of the pyrolysis route is either about the same as or less than the conventional technologies in each of the studied cases. Because of the use of a waste feedstock, MFI analysis shows that the overall aggregate supply chain energy of the modeled mixed plastic pyrolysis plant is 24% lower than the conventional baseline. This is mainly because producing virgin plastic incurs environmental burdens related to fossil-naphtha feedstock.[49] Similar to our study, Jeswani *et al.*[49] demonstrated that chemical recycling of mixed plastic waste by pyrolysis uses 50% less life cycle energy than virgin plastics.

Supply chain GHG emissions, conversely, only include emissions from the combustion of fuel to generate process heat or electricity. Thus, it is largely process specific. Because fossil inputs designated as feedstocks are, by definition, not combusted, they do not exhibit associated GHG emissions. Furthermore, because the transportation distance is considered to be less than 180 kilometers, the overall contributions from transportation are smaller for the pyrolysis-based process.

Across all case studies, pyrolysis utilizes waste plastic rather than fossil fuels as its feedstock and therefore exhibits low (in some cases negative) fossil fuel depletion in LCA (Fig. 7a–h and Tables S23–S26, ESI†), in agreement with the MFI supply chain energy results. The technology also emits less chlorine, bromine, nitrogen, volatile organic compounds (VOCs) and NO*x* than fossil-derived naphtha or BTX mixture, resulting in lower or statistically equivalent acidification, ozone depletion, and smog formation potentials for most cases (excepting Case D – ethylene). However, high plastic feedstock and utility (electricity, refrigeration, steam) requirements per unit product result in poorer performance than the corresponding virgin materials across most other metrics. Potential areas for process improvement therefore include eliminating the energy-intensive plastic flaking process, co-locating the pyrolysis plant with a MRF to reduce transportation impacts, increasing yields, and incorporating further heat/energy integration. For example, Case C – in which BTX aromatics yield is maximized using a catalyst with high aromatics selectivity – offers a promising route to decrease both environmental impacts and MSP. Avoided emissions also play a crucial role in lowering the environmental impacts of pyrolysis in Cases B–D; it is therefore essential to efficiently capture and utilize all co- products.

Conclusions

Herein we evaluated four fast pyrolysis process designs for recycling mixed plastic wastes from a techno-economic and life cycle perspective. We discuss key drivers that have major impacts on process economics, supply chain energy, GHG emissions, and environmental sustainability. Specifically, the TEA results of our first process design estimate the MSP of naphtha to be four times that of its fossil counterpart. Feedstock cost and utilities were two of the major cost drivers. In a second design, which is our base case, the pyrolysis effluent stream underwent rigorous purification to recover high-value products (olefins, aromatics, natural gas liquids, and naphtha). The revenue from the sale of multiple coproducts offsets overall project costs and estimate BTX aromatic hydrocarbon production at $1.07/kg, which is 1.6-times that of fossil BTX product. Further, two more scenarios selectively produce more aromatics and olefins products. Both cases are estimated to exhibit an MSP of BTX aromatic compounds and ethylene monomer closer to their fossil counterparts. A multivariate sensitivity analysis was performed to anticipate future uncertainties in the context of the crude oil price. The analysis indicates that pyrolysis-based refineries can attain cost-competitiveness with petroleum manufacturing processes when the price of crude oil increases ($>$ $60/bbl). The environmental implications of all four process designs were quantified using the MFI tool and LCA, which show that the utilization of waste plastic feedstock results in a reduction in supply chain energy use and fossil fuel depletion in all four processes. However, all cases show increases in GHG emissions and LCA impact categories such as carcinogenics, ecotoxicity, eutrophication, respiratory effects, and water use. These poor results are associated with feedstock pretreatment requirements and the use of process utilities such as steam, methane, and electricity. Overall, this study highlights the use of transparent and comprehensive TEA/LCA for understanding the emerging chemical recycling landscape.

Conflicts of interest

None to declare.

Acknowledgements

This work was authored in part by the National Renewable Energy Laboratory, operated by Alliance for Sustainable Energy, LLC, for the U.S. Department of Energy (DOE) under contract no. DE-AC36-08GO28308. Funding was provided by the US Department of Energy, Office of Energy Efficiency and Renewable Energy, Advanced Manufacturing Office, and Bioenergy Technologies Office. This work was performed as part of the Bio-Optimized Technologies to keep Thermoplastics out of Landfills and the Environment (BOTTLE) Consortium. The BOTTLE Consortium includes members from MIT, funded under Contract DE-AC36-08GO28308 with NREL. The views expressed in the article do not necessarily represent the views of the DOE or the U.S. Government. The U.S. Government retains and the publisher, by accepting the article for publication, acknowledges that the U.S. Government retains a non-exclusive, paid-up, irrevocable, worldwide license to publish or reproduce the published form of this work, or allow others to do so, for U.S. Government purposes. We thank our colleagues in the BOTTLE Consortium for their helpful discussions. We would like to extend our special thanks to Kurt Van Allsburg for his help with the CatCost tool, and to Nicholas Carlson and Michael Talmadge for their assistance with petrochemicals pricing in this work.

References

1 S. B. Borrelle, J. Ringma, K. L. Law, C. C. Monnahan, L. Lebreton, A. McGivern, E. Murphy, J. Jambeck, G. H. Leonard and M. A. Hilleary, *Science*, 2020, **369**, 1515–1518.
2 K. L. Law and R. Narayan, *Nat. Rev. Mater.*, 2021, **7**, 104–116.
3 E. Ormonde, M. DeGuzman, M. Yoneyama, U. Loechner and X. Zhu, *Plastics Recycling - Chemical Economics Handbook*, IHS Markit, 2019, **https://ihsmarkit.com/products/plastics-recycling-chemical-economicshandbook.html.)**.
4 M. Kusenberg, A. Eschenbacher, M. R. Djokic, A. Zayoud, K. Ragaert, S. De Meester and K. M. Van Geem, *Waste Manage.*, 2022, **138**, 83–115.
5 H. Li, H. A. Aguirre-Villegas, R. D. Allen, X. Bai, C. H. Benson, G. T. Beckham, S. L. Bradshaw, J. L. Brown, R. C. Brown, V. S. Cecon, J. B. Curley, G. W. Curtzwiler, S. Dong, S. Gaddameedi, J. E. García, I. Hermans, M. S. Kim, J. Ma, L. O. Mark, M. Mavrikakis, O. O. Olafasakin, T. A. Osswald, K. G. Papanikolaou, H. Radhakrishnan, M. A. Sanchez Castillo, K. L. Sánchez-Rivera, K. N. Tumu, R. C. Van Lehn, K. L. Vorst, M. M. Wright, J. Wu, V. M. Zavala, P. Zhou and G. W. Huber, *Green Chem.*, 2022, **24**, 8899–9002.
6 A. Rahimi and J. M. García, *Nat. Rev. Chem.*, 2017, **1**, 0046.
7 K. Ragaert, L. Delva and K. Van Geem, *Waste Manage.*, 2017, **69**, 24–58.
8 G. W. Coates and Y. D. Getzler, *Nat. Rev. Mater.*, 2020, **5**, 501–516.
9 I. Vollmer, M. J. Jenks, M. C. Roelands, R. J. White, T. van Harmelen, P. de Wild, G. P. van Der Laan, F. Meirer, J. T. Keurentjes and B. M. Weckhuysen, *Angew. Chem., Int. Ed.*, 2020, **59**, 15402–15423.
10 L. D. Ellis, N. A. Rorrer, K. P. Sullivan, M. Otto, J. E. McGeehan, Y. Román-Leshkov, N. Wierckx and G. T. Beckham, *Nat. Catal.*, 2021, **4**, 539–556.
11 S. C. Kosloski-Oh, Z. A. Wood, Y. Manjarrez, J. P. De Los Rios and M. E. Fieser, *Mater. Horiz.*, 2021, **8**, 1084–1129.
12 A. J. Martín, C. Mondelli, S. D. Jaydev and J. Pérez-Ramírez, *Chem*, 2021, **7**, 1487–1533.
13 M. Solis and S. Silveira, *Waste Manage.*, 2020, **105**, 128–138.
14 M. Zeller, N. Netsch, F. Richter, H. Leibold and D. Stapf, *Chem. Ing. Tech.*, 2021, **93**, 1763–1770.
15 T. P. Vispute, H. Zhang, A. Sanna, R. Xiao and G. W. Huber, *Science*, 2010, **330**, 1222–1227.
16 S. Orozco, M. Artetxe, G. Lopez, M. Suarez, J. Bilbao and M. Olazar, *ChemSusChem*, 2021, **14**, 4291.
17 R. R. Bora, R. Wang and F. You, *ACS Sustainable Chem. Eng.*, 2020, **8**, 16350–16363.
18 O. Dogu, M. Pelucchi, R. Van de Vijver, P. H. Van Steenberge, D. R. D'hooge, A. Cuoci, M. Mehl, A. Frassoldati, T. Faravelli and K. M. Van Geem, *ACS Sustainable Chem. Eng.*, 2021, **84**, 100901.
19 S. D. Anuar Sharuddin, F. Abnisa, W. M. A. Wan Daud and M. K. Aroua, *Energy Convers. Manage.*, 2016, **115**, 308–326.
20 S. R. Nicholson, J. E. Rorrer, A. Singh, M. O. Konev, N. A. Rorrer, A. C. Carpenter, A. J. Jacobsen, Y. Román-Leshkov and G. T. Beckham, *Annu. Rev. Chem. Biomol. Eng.*, 2022, **13**, 301–324.
21 L. S. Diaz-Silvarrey, K. Zhang and A. N. Phan, *Green Chem.*, 2018, **20**, 1813–1823.
22 A. Marcilla, M. Beltran and R. Navarro, *Ind. Eng. Chem. Res.*, 2008, **47**, 6896–6903.
23 K.-H. Lee and D.-H. Shin, *Waste Manage.*, 2007, **27**, 168–176.
24 A. Lopez, I. De Marco, B. Caballero, M. Laresgoiti and A. Adrados, *Chem. Eng. J.*, 2011, **173**, 62–71.
25 R. K. Singh, B. Ruj, A. Sadhukhan and P. Gupta, *J. Energy Inst.*, 2019, **92**, 1647–1657.
26 F. Sasse and G. Emig, *Chem. Eng. Technol.*, 1998, **21**, 777–789.
27 L. O. Mark, M. C. Cendejas and I. Hermans, *ChemSusChem*, 2020, **13**, 5808–5836.
28 K. Sun, N. J. Themelis, A. T. Bourtsalas and Q. Huang, *J. Cleaner Prod.*, 2020, **268**, 122038.
29 M. Kusenberg, A. Zayoud, M. Roosen, H. D. Thi, M. S. Abbas-Abadi, A. Eschenbacher, U. Kresovic, S. De Meester and K. M. Van Geem, *Fuel Process. Technol.*, 2022, **227**, 107090.
30 Y. Wang, L. Cheng, J. Gu, Y. Zhang, J. Wu, H. Yuan and Y. Chen, *ACS Omega*, 2022, **7**(3), 2752–2765.
31 M.-H. Cho, S.-H. Jung and J.-S. Kim, *Energy Fuels*, 2010, **24**, 1389–1395.
32 A. Eschenbacher, R. J. Varghese, M. S. Abbas-Abadi and K. M. Van Geem, *Chem. Eng. J.*, 2022, **428**, 132087.
33 G. Elordi, M. Olazar, M. Artetxe, P. Castaño and J. Bilbao, *Appl. Catal., A*, 2012, **415**, 89–95.
34 A. Inayat, A. Inayat, W. Schwieger, B. Sokolova and P. Lestinsky, *Fuel*, 2022, **314**, 123071.
35 P. T. Williams, *Feedstock recycling and pyrolysis of waste plastics: converting waste plastics into diesel and other fuels*, 2006, pp. 285–313.
36 N. Miskolczi, L. Bartha and G. Deák, *Polym. Degrad. Stab.*, 2006, **91**, 517–526.
37 W. Ding, J. Liang and L. L. Anderson, *Fuel Process. Technol.*, 1997, **51**, 47–62.
38 H. E. Toraman, T. Dijkmans, M. R. Djokic, K. M. Van Geem and G. B. Marin, *J. Chromatogr. A*, 2014, **1359**, 237–246.
39 W. Kaminsky, B. Schlesselmann and C. Simon, *J. Anal. Appl. Pyrolysis*, 1995, **32**, 19–27.
40 M. Artetxe, G. Lopez, G. Elordi, M. Amutio, J. Bilbao and M. Olazar, *Ind. Eng. Chem. Res.*, 2012, **51**, 13915–13923.
41 C. Simon, W. Kaminsky and B. Schlesselmann, *J. Anal. Appl. Pyrolysis*, 1996, **38**, 75–87.
42 R. Miandad, M. Rehan, M. A. Barakat, A. S. Aburiazaiza, H. Khan, I. M. I. Ismail, J. Dhavamani, J. Gardy, A. Hassanpour and A.-S. Nizami, *Front. Energy Res.*, 2019, **7**, 27.
43 R. K. Verma and T. Pavone, (2017). Process Economics Program Report 300. Unconventional Aromatics Processes (IHS Markit). **https://ihsmarkit.com/products/chemical-technology-pep-300-unconventional-aromatics-processes.html)**.

44 X. Zhao and F. You, *AIChE J.*, 2021, **67**, e17127.
45 U. R. Gracida-Alvarez, O. Winjobi, J. C. Sacramento-Rivero and D. R. Shonnard, *ACS Sustainable Chem. Eng.*, 2019, **7**, 18254–18266.
46 F. Riedewald, Y. Patel, E. Wilson, S. Santos and M. Sousa-Gallagher, *Waste Manage.*, 2021, **120**, 698–707.
47 G. Jiang, J. Wang, S. M. Al-Salem and G. A. Leeke, *Energy Fuels*, 2020, **34**, 7397–7409.
48 A. Fivga and I. Dimitriou, *Energy*, 2018, **149**, 865–874.
49 H. Jeswani, C. Krüger, M. Russ, M. Horlacher, F. Antony, S. Hann and A. Azapagic, *Sci. Total Environ*, 2021, **769**, 144483.
50 S. Das, C. Liang and J. B. Dunn, *Waste Manage.*, 2022, **153**, 81–88.
51 R. J. Hanes and A. Carpenter, *Environ. Syst. Decis.*, 2017, **37**, 6–12.
52 S. Liu, P. A. Kots, B. C. Vance, A. Danielson and D. G. Vlachos, *Sci. Adv.*, 2021, **7**, eabf8283.
53 L. Dai, N. Zhou, Y. Lv, K. Cobb, Y. Cheng, Y. Wang, Y. Liu, P. Chen, R. Zou and H. Lei, *Energy Convers. Manage.*, 2021, **245**, 114578.
54 A. M. Ward, A. J. M. Oprins and R. Narayanaswamy, *US. Pat.*, 2016/0362609 A1, 2016.
55 K. K. Ramamurthy, R. Narayanaswamy, V. R. G. Bhotla, A. Stanislaus and S. Ganji, *US. Pat.*, 0017773, 2020.
56 G. W. Huber, A. M. Gaffney, J. Jae and Y.-T. Cheng, *US. Pat.*, 9169442, 2015.
57 A. Dutta, A. H. Sahir, E. Tan, D. Humbird, L. J. Snowden-Swan, P. A. Meyer, J. Ross, D. Sexton, R. Yap and J. Lukas, *Process Design and Economics for the Conversion of Lignocellulosic Biomass to Hydrocarbon Fuels: Thermochemical Research Pathways with In Situ and Ex Situ Upgrading of Fast Pyrolysis Vapors*, United States, 2015.
58 R. Westerhout, M. Van Koningsbruggen, A. G. Van Der Ham, J. Kuipers and W. P. M. Van Swaaij, *Chem. Eng. Res. Des.*, 1998, **76**, 427–439.
59 J. Sahu, K. Mahalik, H. K. Nam, T. Y. Ling, T. S. Woon, M. S. bin Abdul Rahman, Y. Mohanty, N. Jayakumar and S. Jamuar, *Environ. Prog. Sustainable Energy*, 2014, **33**, 298–307.
60 A. Milbrandt, K. Coney, A. Badgett and G. T. Beckham, *Resour., Conserv. Recycl.*, 2022, **183**, 106363.
61 RecyclingMarkets.net, Secondary Materials Pricing, **https://www.recyclingmarkets.net/**).
62 Brightmark, Press Release. ***https://www.brightmark.com/plastics-renewal/projects/ashley-indiana***, 2021.
63 J. Powell, Resource Recycling, **https://resource-recycling.com/recycling/2018/10/01/sortation-by-the-numbers/**, 2018.
64 M. S. Qureshi, A. Oasmaa, H. Pihkola, I. Deviatkin, A. Tenhunen, J. Mannila, H. Minkkinen, M. Pohjakallio and J. Laine-Ylijoki, *J. Anal. Appl. Pyrolysis*, 2020, **152**, 104804.
65 A. López, I. De Marco, B. Caballero, M. Laresgoiti and A. Adrados, *Fuel Process. Technol.*, 2011, **92**, 253–260.
66 I. C. McNeill, L. Memetea and W. J. Cole, *Polym. Degrad. Stab.*, 1995, **49**, 181–191.
67 R. Narayanaswamy, K. K. Ramamurthy and P. Sreenivasan, *US. Pat.*, 9212318B2, 2015.
68 S. Budsaereechai, A. J. Hunt and Y. Ngernyen, *RSC Adv.*, 2019, **9**, 5844–5857.
69 A. M. Ward, A. J. M. Oprins and R. Narayanaswamy, *US. Pat.*, 0362609, 2019.
70 H. Zimmermann and R. Walzl, *Ullmann's Encyclopedia of Industrial Chemistry*, 2009.
71 A. Liu, in *Handbook of Petroleum Refining Processes*, ed. R. A. Meyers, McGraw-Hill Education, New York, 4th edn, 2016.
72 S. R. Nicholson, *Analyzing Next-generation Supply Chains Using the Materials Flows Through Industry Tool*, National Renewable Energy Lab.(NREL), Golden, CO (United States), 2020.
73 G. Wernet, C. Bauer, B. Steubing, J. Reinhard, E. Moreno-Ruiz and B. Weidema, *Int. J. Life Cycle Assess.*, 2016, **21**, 1218–1230.
74 R. J. Chang and J. Lacson, *Process Economics Tool - PEP Yearbook, IHS Markit*, 2020.
75 M. Talmadge, C. Kinchin, H. Li Chum, A. de Rezende Pinho, M. Biddy, M. B. B. de Almeida and L. Carlos Casavechia, *Fuel*, 2021, **293**, 119960.
76 S.-H. Jung, M.-H. Cho, B.-S. Kang and J.-S. Kim, *Fuel Process. Technol.*, 2010, **91**, 277–284.
77 N. A. Rorrer, S. Nicholson, A. Carpenter, M. J. Biddy, N. J. Grundl and G. T. Beckham, *Joule*, 2019, **3**, 1006–1027.
78 J. Bare, *Clean Technol. Environ. Policy*, 2011, **13**, 687–696.
79 AWARE, (Available WAter REmaining) Mission and Goals - WULCA **https://wulca-waterlca.org/aware/**, (accessed 21 March 2022).
80 F. Associates, Life cycle impacts for postconsumer recycled resins: PET, HDPE, and PP. Overland Park, 2018. **https://plasticsrecycling.org/images/library/2018-APR-LCI-report.pdf** (accessed on Nov. 2021).
81 J. C. Bare, *J. Ind. Ecol.*, 2002, **6**, 49–78.
82 T. Hundertmark, M. Prieto, A. Ryba, T. J. Simons and J. Wallach, Accelerating plastic recovery in the United States. **https://www.mckinsey.com/industries/chemicals/our-insights/accelerating-plastic-recovery-in-the-united-states).**
83 J. Scheirs and W. Kaminsky, *Feedstock recycling and pyrolysis of waste plastics: converting waste plastics into diesel and other fuels*, John Wiley & Sons Incorporated, 2006.
84 S. H. Gebre, M. G. Sendeku and M. Bahri, *ChemistryOpen*, 2021, **10**, 1202–1226.
85 A. Buekens, *Conserv. Recycl.*, 1977, **1**, 247–271.
86 M. Kusenberg, M. Roosen, A. Zayoud, M. R. Djokic, H. D. Thi, S. De Meester, K. Ragaert, U. Kresovic and K. M. Van Geem, *Waste Manage.*, 2022, **141**, 104–114.
87 S. Li, I. Cañete Vela, M. Järvinen and M. Seemann, *Waste Manage.*, 2021, **130**, 117–126.
88 A. Zayoud, H. D. Thi, M. Kusenberg, A. Eschenbacher, U. Kresovic, N. Alderweireldt, M. R. Djokic and K. Van Geem, *Waste Manage.*, 2022, **139**, 85–95.
89 H. Dao Thi, M. R. Djokic and K. M. Van Geem, *Separations*, 2021, **8**, 103.

90 M. Larrain, S. Van Passel, G. Thomassen, U. Kresovic, N. Alderweireldt, E. Moerman and P. Billen, *J. Cleaner Prod.*, 2020, **270**, 122442.
91 J. Goyal, Large-scale Pyrolysis—Plastic Chemical Recycling. Process Economics Program Report 199G (IHS Markit). **https://www.spglobal.com/commodityinsights/en/ci/products/large-scale-pyrolysis-plastic-chemical-recycling.html)**.
92 D. Porshnov, *Wiley Interdiscip. Rev.: Energy Environ.*, 2022, **11**, e421.
93 M. Roosen, N. Mys, K. Kleinhans, I. S. Lase, S. Huysveld, M. Brouwer, E. U. T. van Velzen, K. M. Van Geem, J. Dewulf and K. Ragaert, *Resour., Conserv. Recycl.*, 2022, **178**, 106025.
94 A. Aitani, T. Yoshikawa and T. Ino, *Catal. Today*, 2000, **60**, 111–117.
95 G. Lopez, M. Artetxe, M. Amutio, J. Bilbao and M. Olazar, *Renewable Sustainable Energy Rev.*, 2017, **73**, 346–368.
96 D. K. Ratnasari, M. A. Nahil and P. T. Williams, *J. Anal. Appl. Pyrolysis*, 2017, **124**, 631–637.
97 J. Nishino, M. Itoh, H. Fujiyoshi and Y. Uemichi, *Fuel*, 2008, **87**, 3681–3686.
98 K. Sun, Q. Huang, X. Meng, Y. Chi and J. Yan, *Energy Fuels*, 2018, **32**, 9772–9781.
99 P. Dufresne, *Appl. Catal., A*, 2007, **322**, 67–75.
100 B. Luna-Murillo, M. Pala, A. L. Paioni, M. Baldus, F. Ronsse, W. Prins, P. C. Bruijnincx and B. M. Weckhuysen, *ACS Sustainable Chem. Eng.*, 2020, **9**, 291–304.
101 I. Velghe, R. Carleer, J. Yperman and S. Schreurs, *J. Anal. Appl. Pyrolysis*, 2011, **92**, 366–375.
102 A.-S. Bescond and K. Smith, *Chemical Economics Handbook*, IHS Markit, 2021.
103 J. P. Tilsted, A. Mah, T. D. Nielsen, G. Finkill and F. Bauer, *Energy Res. Soc. Sci.*, 2022, **94**, 102880.
104 M. Kusenberg, G. C. Faussone, H. D. Thi, M. Roosen, M. Grilc, A. Eschenbacher, S. De Meester and K. M. Van Geem, *Sci. Total Environ.*, 2022, 156092.
105 M. S. Mettler, D. G. Vlachos and P. J. Dauenhauer, *Energy Environ. Sci.*, 2012, **5**, 7797–7809.
106 S. R. Nicholson, N. A. Rorrer, A. C. Carpenter and G. T. Beckham, *Joule*, 2021, **5**, 673–686.
107 A. Singh, N. A. Rorrer, S. R. Nicholson, E. Erickson, J. S. DesVeaux, A. F. T. Avelino, P. Lamers, A. Bhatt, Y. Zhang, G. Avery, L. Tao, A. R. Pickford, A. C. Carpenter, J. E. McGeehan and G. T. Beckham, *Joule*, 2021, **5**, 2479–2503.